Mineral granulometric analysis using mathematical morphology

Jonathas Barbosa
jonathasbarbosa@gmail.com

JanKees van der Poel
jkvdpoel@yahoo.com.br
Universidade Federal da
Paraíba
PPGEM/DEM/CT

Leonardo Vidal Batista
leonardo@di.ufpb.br
PPGEM/DEM/CT
PPGI/DI/CCEN
Universidade Federal da
Paraíba

Belarmino Barbosa Lira
belarminoblira@yahoo.com.br
Departamento de Engenharia
Civil e Ambiental
SIUSP/UFPB
Universidade Federal da
Paraíba

Abstract

The most accurate granulometric analysis techniques present some disadvantages, mainly related with high cost of acquisition and maintenance of sophisticated devices. On the other hand, cheaper systems are generally characterized by low precision or long time to conclude the analysis. The only techniques capable of conducting a morphological analysis, today considered fundamental to mineral characterization, are image based, generally by microscopy. The main objectives of this paper consist on comparing different image acquisition devices and evaluating the feasibility of using mathematical morphology analysis to obtain granulometric profiles. Each configuration for image acquisition devices proved useful in specific ranges of particle sizes. Computational sieving by mathematical morphology also achieved promising results, and was even capable of discriminating grain sizes of particles trapped in a given physical sieve, thus enhancing granulometric precision.

Keywords: Mineral granulometry. Mathematical Morphology. Computer vision.

1 Introduction

Computerized image analysis, or Computer Vision, has been widely used to characterize particles' size and morphology [1][2][3][4][7][10][15]. Computer Vision techniques based on Mathematical Morphology are also being increasingly adopted in many sectors (such as pharmaceutical, biotechnology, ceramics, polymers, pigments, abrasives and explosives industries), as they allow further investigation of relevant phenomena such as particle's clustering tendency and impure particles detection.

Techniques based on technologically sophisticated devices have high costs, mainly associated with equipment purchasing and maintenance and also, in many cases, with problems associated by using ionizing radiation (Gamma and X Rays). Cheaper systems, moreover, often require the use of thermally insulated drying chambers, which means more time to obtain results, and are characterized by low accuracy in determining the granulometric profile. In almost all cases, the analysis time depends on the granulometric range that will be analyzed and on the accuracy required. In other words, the higher the accuracy, the more time is needed for the analysis, which can reach up to 24 hours.

The goal of this paper is to investigate the feasibility of using computational image analysis techniques to obtaining a granulometric profile. This method has the advantages of having no subjectivity, as well as a reduced cost when compared to the laser diffraction method. The rest of the paper is organized as follows: Section 2 gives a brief description of materials

116

Rev. Tecnol. Fortaleza, v. 32, n. 1, p. 116-126, jun. 2011.

and methods used in this work; Section 3 presents the results obtained by means of computational sieving; and Section 4 discusses and concludes the paper.

2. Materials and methods

This section describes the materials and methods that enabled the realization of this study, as well as to substantiate the concepts and tools used in it.

2.1 Classification by Sieving

One of the oldest techniques for particle classification—the separation based on the sample size or any other of its physical attributes — and still widely used today is sieving. The preponderance of this method is due to some of its advantages, such as low investment cost, relative ease of implementation and execution (which, in turn, requires low technical skills), good reliability and capability to separate particles in sizes that vary from 100mm to 0.02mm [9][11] [12][13]. These characteristics are not usually associated with other classification methods.

The series of sieves used in this work was the Tyler Series.

2.2 Image Acquisition

Image capture for processing and analysis was performed by means of a Photographic Camera Canon EOS Digital SLR Camera – Rebel XTi, a Trinocular Stereoscopic Microscope Taimin XTB-1B and a Table Scanner Microtek ScanMaker i800. Using these three devices, four methods of image acquisition were tested: 1. the photographic camera equipped with a 50mm objective; 2. the photographic camera equipped with macro lens; 3. the microscope with a photographic camera attached to it; and 4. the table scanner.

Being in possession of such equipment and of the ore samples, the next step was to define the useful viewing range for each device and its associations. This range was set from two items: 1. the apparatus physical feasibility; and 2. its field of view in the captured image.

Verifying the apparatus physical feasibility consists on checking if it is possible to capture the image of a specific grain size with a certain device or association of devices. For example, it is impossible to use the scanner to capture images of grains larger than 1.5 mm (mesh number 12, 8 and 4) because the lid of the scanner will not closed due to the grain size. The field of view is very restricted, for example, in the camera with microscope association. In this case, capturing grains larger than 600μm (meshes number 30, 20, 16, 12, 8 and 4) involves viewing only a few grains fully contained in the image, reducing the granulometry reliability (Francus, 2005). In Table 1 one can verify the useful particle visualization range. In this table, "P.C. 50mm" means the photographic camera with 50mm lenses, "P.C. Macro" means the photographic camera with macro lenses e "P.C. + Mic." means the association of the photographic camera with the microscope.

Table 1: Useful particle visualization range.

Mesh	P.C. 50mm	P.C. Macro	P.C. + Mic.	Scanner
4	X			
8	X			
12	X			
16	X			X
20	X	X		X
30	X	X		X
40		X	X	X
50		X	X	X
70		X	X	X
100		X	X	X
140		X	X	X
270		X	X	X
400			X	

2.3 Morphological Operations

To extract components of interest in a digital image is one of the fundamental problems in the image processing and analysis field [8]. Regarding the image processing and computer vision, Mathematical Morphology is used as a tool to extract components of an image that are useful in representing and describing its shape, such as borders (or frontiers), circularity, convexity, ellipticity, convex hull and symmetry[14].

As will be seen next, the main idea of studying Mathematical Morphology is to extract information on the geometry and topology of an unknown set (or ensemble), that is, an image, and compare this information with a well-defined set called **structuring element** [5][6]. There are linear, circular and composed structural elements.

Dilation and *erosion* are the most used morphological operators. From them, other morphological operations of greater complexity (opening and closing) can be expressed, providing interesting and useful results in image processing.

2.4. Morphological and Physical Sieving

To estimate the relationship between the mass retained in the manual and computer sieving, it was used the equation that relates mass and volume, $m = \rho V$, where ρ is the ore density — or specific mass. As the computational sieving was performed with a disc-shaped structural element, by knowing the number of particles with a given radius r it is possible to approximate the ore weight for that specific particle area or volume.

Thus, the procedure followed was: 1. Calculating the relationship between the mass of the product obtained by manual sieving; 2. Computational separation followed by counting the grains retained in each computational mesh; 3. Determination of the size of the division between the sieves (the cutting radius) 4. Grain area and volume approximation.

In order to summarize the steps of this method the block diagram is presented in Figure 1. The whole sequence will be illustrated in detail in section 3.
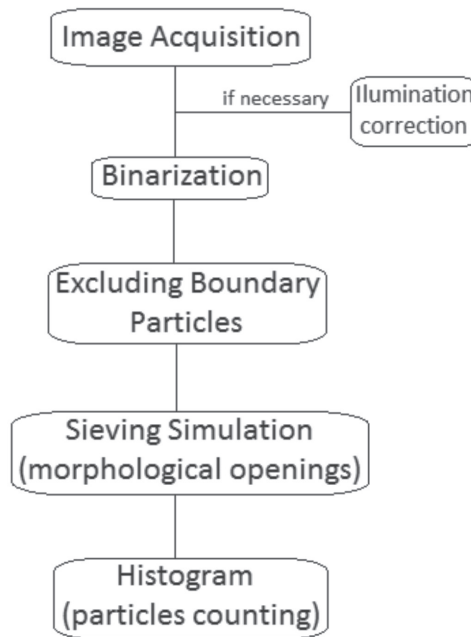
Figure 1: Block diagram since image acquisition until particles counting.

3 Results

This section presents the results concerning the display range of all equipments used in the image acquisition and the Mathematical Morphology sieving. It also compares manual and digital sieving methods. The results of lighting correction in the images captured with the macro lens are shown in Subsection 3.2. As shown before, Table 1 gives the useful particle visualization ranges for each image acquisition method used in this work.

3.1 Computational Sieving Using Mathematical Morphology

The processing steps involved in the computational sieving method using Mathematical Morphology will be illustrated based on two example images, each one captured with a different instrument. The first image was captured with a camera equipped with 50mm lenses (its standard lenses) and the second one was captured with a scanner. Both images are preprocessed by means of a binarization operation.

For each image, charts with the particle size distribution, histograms representing the number of grains versus the amount of pixels found, and images that show the amount of material withheld in each computational sieving stage are given. In the end, a comparison between the manual and computational sieving is done.

There is also a third example image, captured with a camera equipped with macro lenses, that is shown in order to emphasize illumination correction preprocessing.

Camera with 50mm lenses: grains on Figure 2 are obtained from the junction of ore samples retained in sieves with meshes 12 and 16.

(a)   (b)
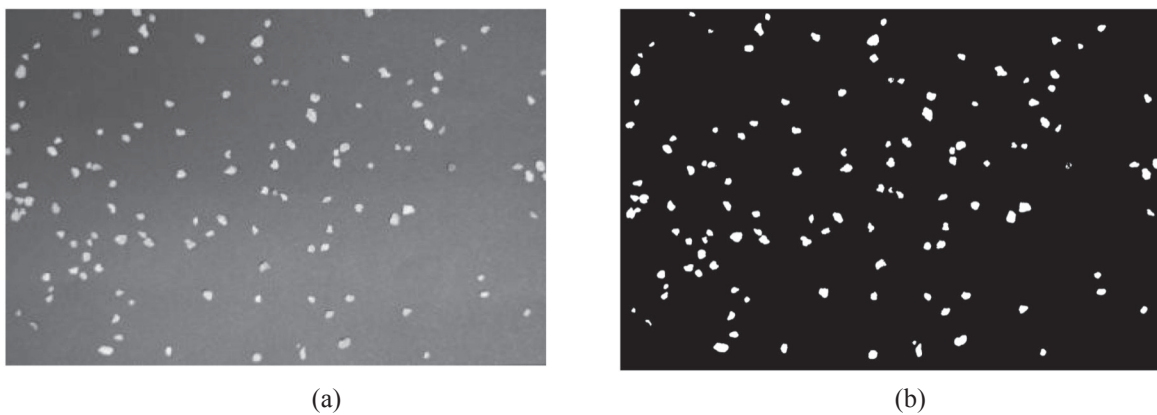
Figure 2: Junction of sieves with meshes 12 and 16: (a) gray scale image (original); (b) enhanced and binarized image, without objects at the edges.

Figure 3a represents the computational sieving. Image objects are sifted by opening the image with a structuring element of increasing size and by counting the remaining intensity surface area (the summation of pixel values in the image) after each opening.

In Figure 3b the first derivative is computed and it is possible to see variations in the number of pixels between two consecutive opening operations. A significant variation between two consecutive opening operations indicates the image has objects of the same size of the structuring element used in the smaller opening operation.

(a)   (b)
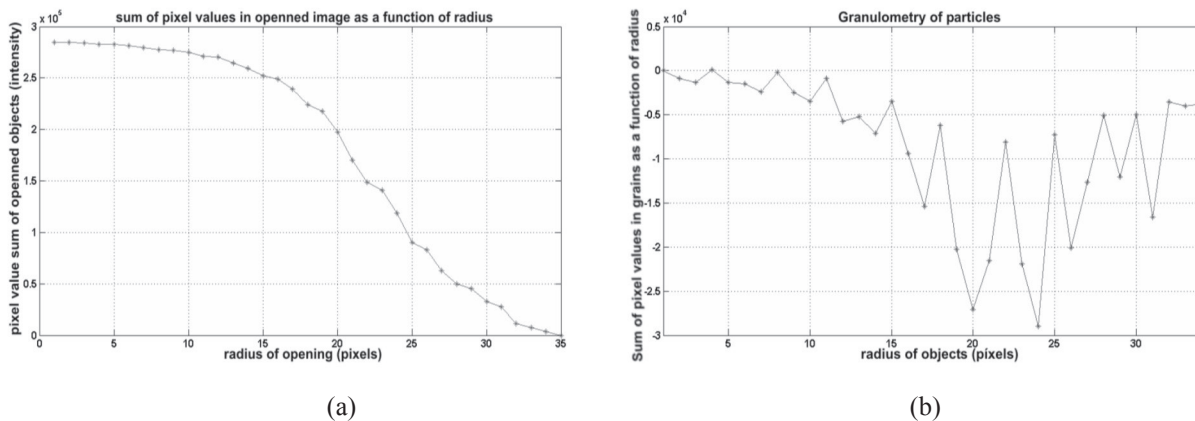
Figure 3: (a) Computational sieving simulation; (b) Computational variation of grain sizes between sieves.

The histogram shown in Figure 4 results from the grain counting computational process. Its horizontal axis indicates the number of pixels and its vertical axis represents the amount of grains. According to the computational counting in

Figure 2b, there are 123 grains. Computationally counting the grains agrees with visual counting. Even grains that are touching each other were separately counted by morphological sieving.
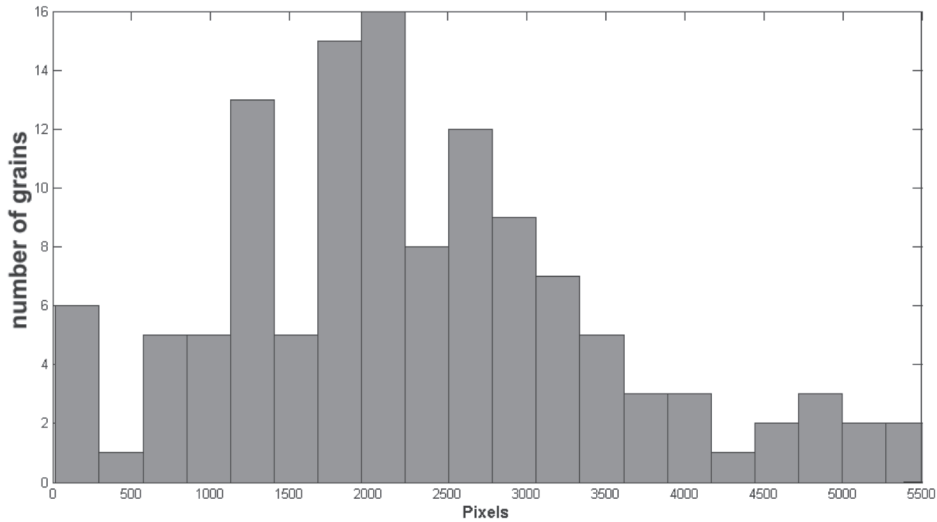
Figure 4: Histogram of grain counting — 123 grains.

Figure 5 displays the result of successive morphological openings as an example of computational sieving. What is seen in (a) is the result of a morphological opening operation with a structuring element of radius 23 and in (b) with a structuring element of radius 24.

(a)   (b)
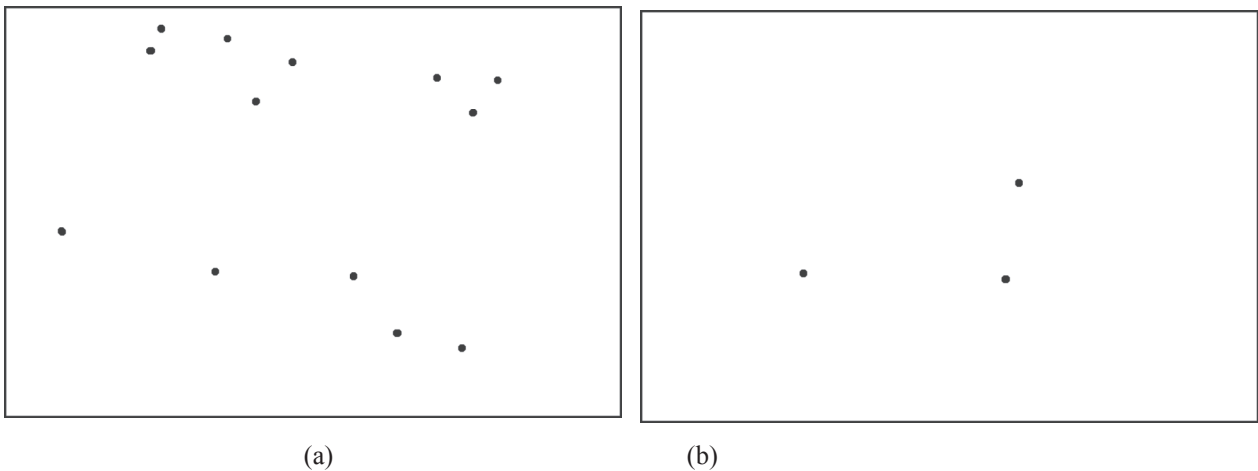
Figure 5: Ore retained in computational sieves. Grains with radius (a) 23, and (b) 24, respectively.

The relationship between manual and computational sieving for the sample in Figure 2 is given by the ratio between the masses of the product in sieves 12 and 16, that is:

- Ratio between the product mass in the sieves: m16/m12 = 91, 71g/102, 16g = 0, 90;
- Ratio between the estimate of the product mass in the sieves (approximation by their area): m16/m12 = 119,026/167, 605 = 0, 71;
- Ratio between the estimate of the product mass in the sieves (approximation by their volume): m16/m12 = 165, 390/330,836 = 0, 50.

Table 2 shows the number of particles according each structure element chose to separate the particles of Figure 2.

**Table 2:** Number of particles in each radius of Figure 2 — 1mm = 26 pixels.

Radius(pixels)	11	12	13	14	15	16	17	18	19	20	21
Particles(number)	4	2	2	3	4	9	3	10	14	11	4
Radius(pixels)	22	23	24	25	26	27	28	29	30	31	-
Particles(number)	9	13	3	8	4	1	4	1	1	1	-

Scanner with 600dpi resolution: grains on Figure 6 are obtained from the junction of ore samples retained in sieves with meshes 40 and 50.

(a)   (b)
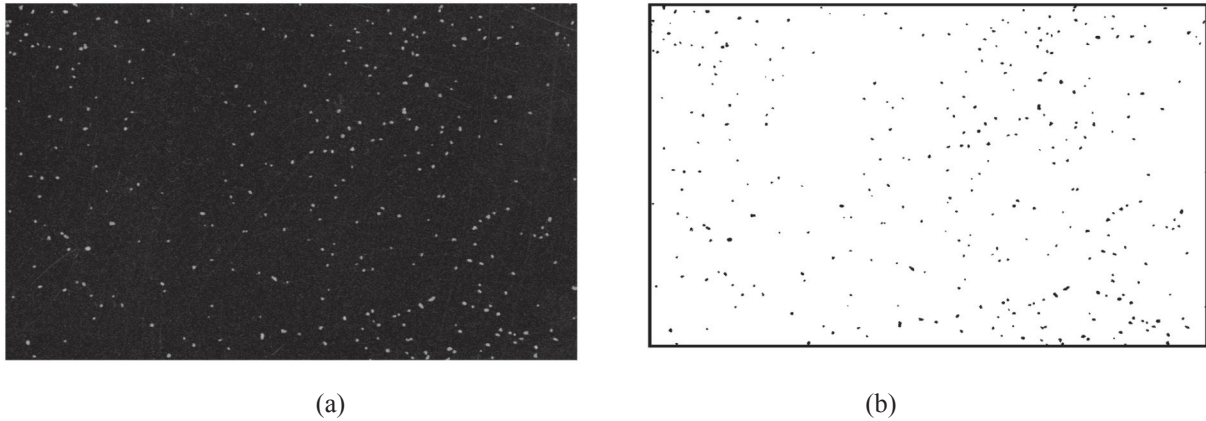
Figure 6: Junction of meshes 40 and 50: (a) gray scale image (original); (b) enhanced and binarized image, without objects at the edges.

The histogram shown in Figure 7 results from the grain counting computational process. According to the computational counting, in Figure 6b there are 319 grains. Again, computationally counting the grains agrees with the visual counting.
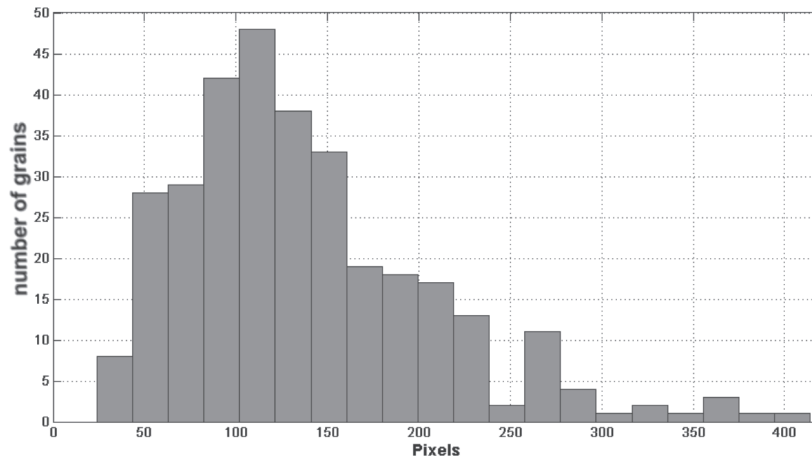
Figure 7: Histogram of grain counting — 319 grains.

The morphological opening operation and the variation in the number of grains between two consecutive opening operations from Figure 6a are shown in Figure 8. In Figure 8a, one can verify that the variation in the structuring element radius was in a range between three and ten. In Figure 8b the variation on the amount of remaining grains can be verified.

Figure 9 shows the separation of the grains from Figure 6a based on morphological opening and reconstruction operations. In Figure 9i there are no grains, which means that in this specific image there are no objects with a size bigger than the structuring element of radius 11.

The relationship between manual and computational sieving for the sample in Figure 6 is given by the ratio between the masses of the product in the sieves 40 and 50, that is:

- Ratio between the product mass in the sieves: m50/m40 = 38, 52g/50, 94g = 0, 756;
- Ratio between the estimate of the product mass in the sieves (approximation by their area): m50/m40 = 8,507/ 7, 57 = 1, 124;
- Ratio between the estimate of the product mass in the sieves (approximation by their volume): m50/m40 = 1,696/2, 123 = 0, 799.

The next Table 3 show detailed the number of particles in each radius of structure element.

Table 3: Number of particles in each radius of the Figure 6 — 1mm = 23.62 pixels.

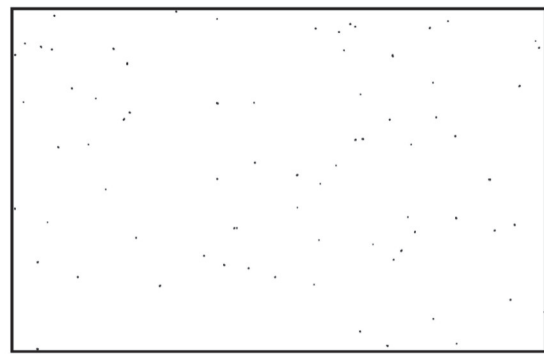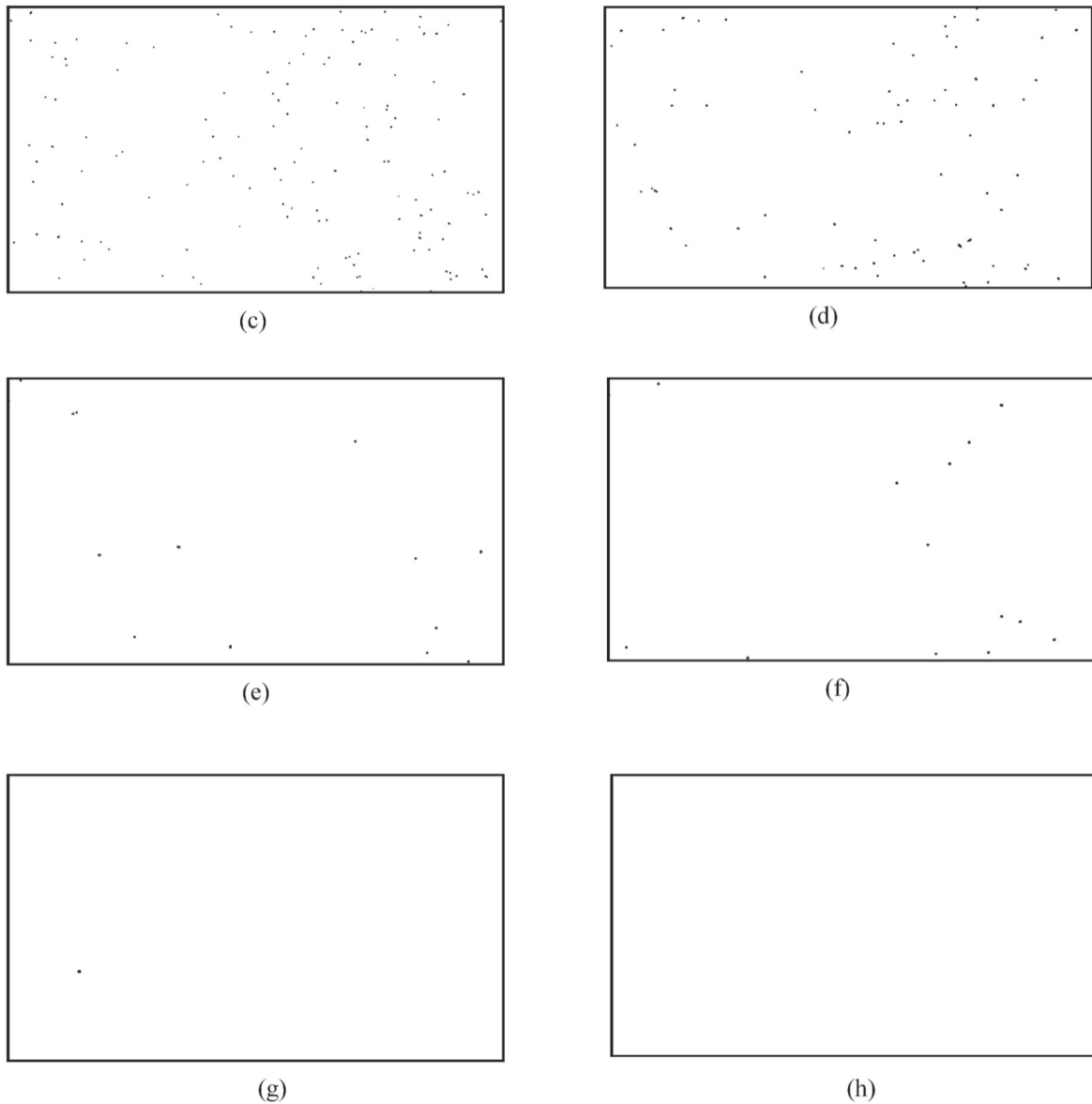| Radius(pixels)	2	3	4	5	6
Particles(number)	10	6	74	138	71
Radius(pixels)	7	8	9	10	-
Particles(number)	14	14	1	0	-

FALTA FIGURA NO ORIGINAL

(a)   (b)
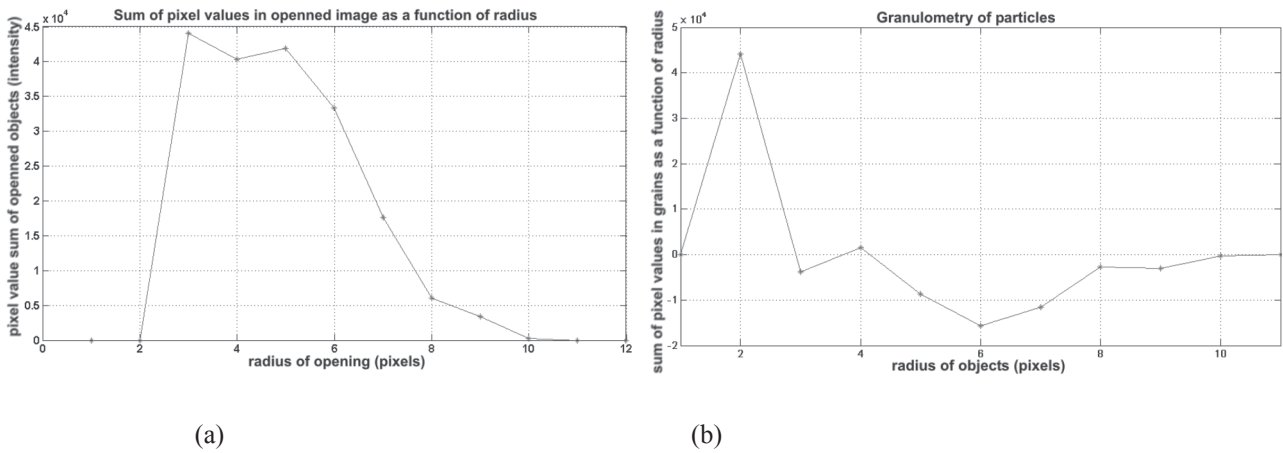
Figure 8: (a) Opening operation radius in the image; (b) Variation of the amount of grains in each opening operation.

a)   b)

122

Rev. Tecnol. Fortaleza, v. 32, n. 1, p. 116-126, jun. 2011.

(c)


(d)

(e)

(f)

(g)

(h)
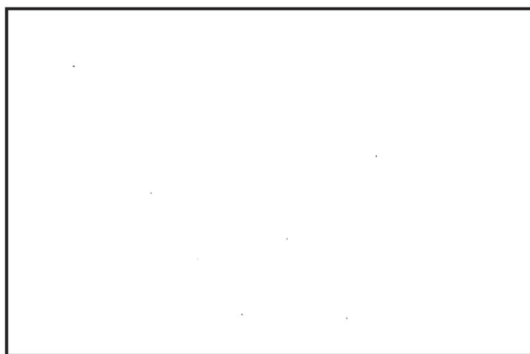
Figure 9: Ore retained in computational sieves: from (a) to (g) grains with radius from three to ten pixels, respectively; (h) image without grains.

3.2 Illumination Correction Preprocessing

It is common to use some kind of preprocessing task to correct certain elements in digital images. Illumination correcting is one of those tasks. In the specific case of acquiring an image with a combination of lenses (macro lenses), the images suffer from an effect that makes their edges to shade off gradually, that is, there is a difference in illumination between the center and the edges of the images, as shown in Figure 10a.

Camera with macro lenses: Figure 10a represents an ore sample retained in sieve 140, and Figure 10b is the binarized image after the preprocessing stage shown in Figure 11.

(a)   (b)
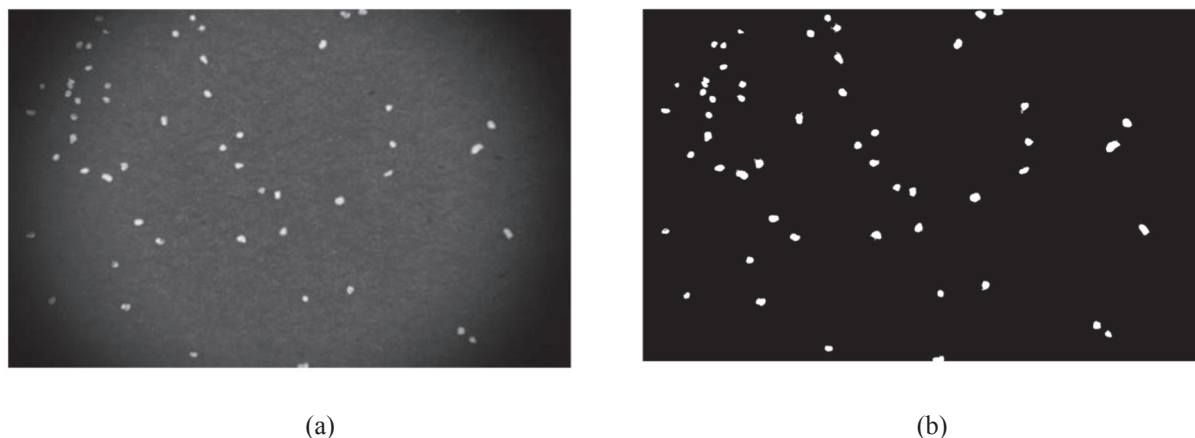
Figure 10: (a) Sample obtained from the sieve 140; (b) Its binarized image.

To enhance contrast in Figure 10a histogram equalization was performed, followed by applying the *imadjust* function in Matlab®, which enhances the image. Next, the morphological opening operation is applied using a structuring element with an adequate radius in order to eliminate small objects (the shield noise) that may remain in the image. In the example image shown here, the structuring element used a 12 pixel radius. The result can be seen in Figure 11. Finally, the image was binarized by adjusting its whitening balance. In this case, a 20% of whitening was used, resulting in what can be seen in the Figure 10b.
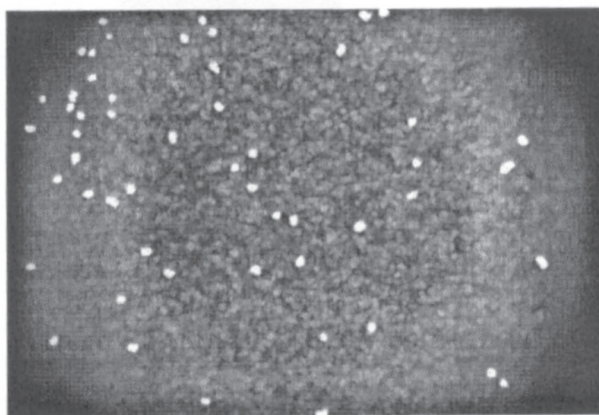
Figure 11: Image Enhancement, histogram equalization and morphological opening on Figure 10a.

Although these elements were brought together by a single physical sieve, the computerized method computer identifies different grain sizes. This means that it is possible to operate with "computational sieves" between the values of the physical sieves. The charts shown in Figures 12a and 12b are related to the opening operations and to the grain size variation relatives to the Figure 10a. It can be seen that from radius 12 there was a sharper decrease in the number of pixels of the image. So from this point one should carry out in the division of the sizes of objects in the image.

Figure 13 is the visualization of the number of grains versus the number of pixels (in other words, the grain counting). According to the computational counting, Figure 10a shows 52 grains.
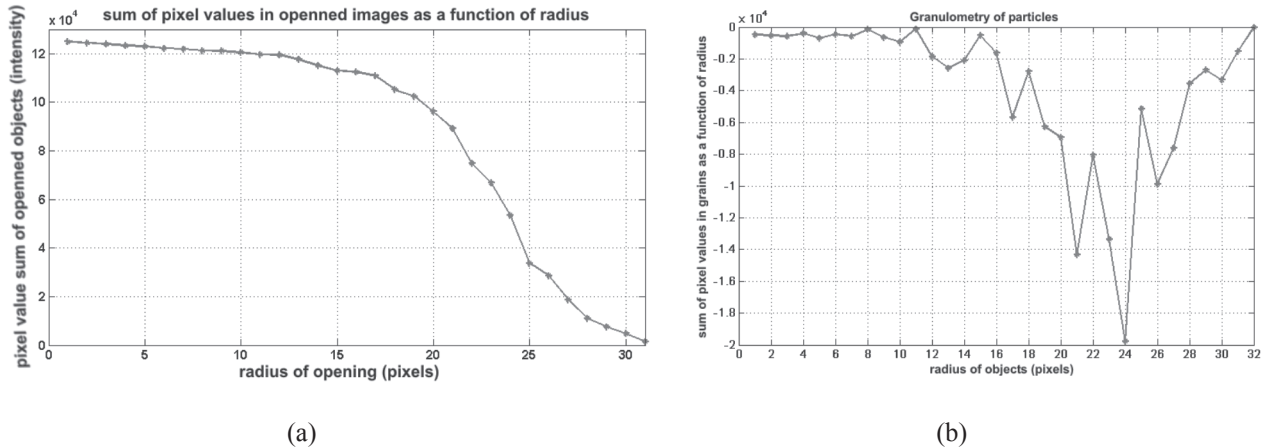
(a)

(b)

Figure 12: (a) Opening radius in the image; (b) Variation on the amount of grains in each opening.
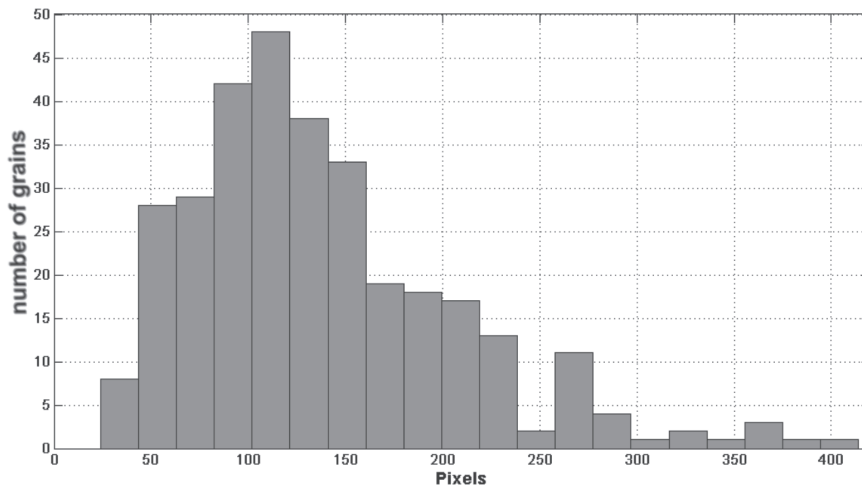

Figure 13: Grain counting histogram — 52 grains.

4 Discussions and conclusions

Computational granulometry by means of Mathematical Morphology shows promising results as it is able to efficiently separate mineral particles of different sizes, as shown in Table 1. Comparing the results obtained with morphologic sieving and physical sieving reveals some discrepancies. This is mainly due to sieving errors and the two dimensional ore image analysis. The ore particles tend to stabilize in the lower energy position, therefore, a simple two dimensional analysis is not sufficient for an accurate prediction. The assumption of spherical particles, common in size profile determination by physical or morphological sieving proved to be inadequate.

Regarding to the equipment used, in the case of the camera and microscope association, the useful range extends beyond a 400 mesh sieve (in other words, it is possible to capture images with quality in which the grains are smaller than 38 micrometers). The same occurs with the scanner, in which its useful range of view is beyond a 400 mesh sieve. However, acquiring images by means of the scanner was difficult because it was necessary to protect it from the ore particles so there was no damage to the device (thus, in this case the particles were arranged on a transparency over the scanner glass). With meshes up to 270, the images were satisfactory, but when 400 mesh was reached, the captured images were also showing the imperfections in the plastic, giving an appearance of an image without focus. This does not occur, or at least was not perceived below 270 mesh.

Concluding, the results show in this paper stated that even when it is necessary to separate elements trapped in a sieve, the computational method is able to identify different grain sizes. This means that it is possible to introduce

different computer sieves between the physical mesh values. This is of great importance when there is a need for greater accuracy in the analysis.

References

AJIT JILLAVENKATESA, A.; DAPKUNAS, S. J.; LUM, Lin-Sien H. *Materials Science and Engineering Laboratory.* Washington, DC: NIST, 2001.

ALLEN, T. *Particle size measurement*: powder sampling and particle size measurement. 5th ed. Delaware, USA: Chapman & Hall, 1997. v. 1

APTOULA, E.; S. LEFÈVRE. A comparative study on multivariate mathematical morphology. *Pattern Recognition*, New York, v. 40, n. 11, p. 2914 -2929, Nov. 2007.

BALAGURUNATHAN, Y. et al. Morphological granulometric analysis of sediment images. *Image Analysis and Stereology,* Slovenia, v. 20, p. 87-99, 2001.

BATMAN, S.; DOUGHERTY, E. R. Size distributions for multivariate morphological granulometries: texture classification and statistical properties. *Optical Engineering* , Slovenia, v. 36, p. 1518–1529, 1997.

DOUGHERTY, E. R. *An introduction to morphological image processing.* Bellingham, WA: SPIE Press, 1992.

FERRARI, S.; PIURI, V.; SCOTTI, F. Virtual environment for granulometry analysis. In: IEEE INTERNATIONAL CONFERENCE ON VIRTUAL ENVIRONMENTS, HUMAN-COMPUTER INTERFACES, AND MEASUREMENT SYSTEMS, 2008, Instambul. *Proceedings*... Instambul, 2008. p. 156-161.

FRANCUS, P. *Image analysis, sediments and paleoenvironments*. Dordrecht: Kluwer Academic Publishers, 1984. (Developments in Paleoenvironmental Research Series).

IGATHINATHANE, C.; PORDESIMO, L. O.; BATCHELOR, W. D. *Ground biomass sieve analysis simulation by image processing and experimental verification of particle size distribution*. St. Joseph, MI: ASABE, 2008a. (ASABE Paper No. 084126).

IGATHINATHANE, C. et al. Shape identification and particles size distribution from basic shape parameters using ImageJ. *Computers and Electronics in Agriculture,* v. 63, n. 2, p. 168-182, 2008.

IGATHINATHANE, C. et al. Sieveless particle size distribution analysis of particulate materials through computer vision. *Computers and Electronics in Agriculture*, v. 66, n. 2, p 147-158, 2009.

KELLY, E. G.; SPOTTIWOOD, D. J. *Introduction to mineral processing*. New York: Wiley, 1982.

SILVA, E. M. et al. Comparação de modelos matemáticos para o traçado de curvas granulométricas. *Pesq. Agropec. Bras.*, Brasília, DF, v. 39, n. 4, p. 363-370, 2004.

VINCENT, L.; DOUGHERTY, E. R. Morphological segmentation for textures and particles. In: DOUGHERTY, E. R. (Ed.). *Digital image processing methods*. New York: Marcel Dekker, 1994. p. 43-102

WOJNAR, L. *Image analysis*: applications in materials engineering. Cracow: CRC Press, 1999.